ER-resident proteins PDR2 and LPR1 mediate the developmental response of root meristems to phosphate availability

Carla A. Ticconi[a], Rocco D. Lucero[a], Siriwat Sakhonwasee[a], Aaron W. Adamson[a], Audrey Creff[b], Laurent Nussaume[b], Thierry Desnos[b], and Steffen Abel[a,c,1]

[a]Department of Plant Sciences, University of California, One Shields Avenue, Davis, CA 95616; [b]Laboratoire de Biologie du Développement des Plantes, Commisariat a l'Energie Atomique Cadarache, 13108 St Paul-lez-Durance, Cedex, France; and [c]Leibniz Institute of Plant Biochemistry, Weinberg 3, D-06120 Halle, Germany

Edited by Richard M. Amasino, University of Wisconsin, Madison, WI, and approved June 30, 2009 (received for review February 18, 2009)

Inadequate availability of inorganic phosphate (Pi) in the rhizosphere is a common challenge to plants, which activate metabolic and developmental responses to maximize Pi acquisition. The sensory mechanisms that monitor environmental Pi status and regulate root growth via altered meristem activity are unknown. Here, we show that *PHOSPHATE DEFICIENCY RESPONSE 2* (*PDR2*) encodes the single P_5-type ATPase of *Arabidopsis thaliana*. PDR2 functions in the endoplasmic reticulum (ER) and is required for proper expression of SCARECROW (SCR), a key regulator of root patterning, and for stem-cell maintenance in Pi-deprived roots. We further show that the multicopper oxidase encoded by *LOW PHOSPHATE ROOT 1* (*LPR1*) is targeted to the ER and that *LPR1* and *PDR2* interact genetically. Because the expression domains of both genes overlap in the stem-cell niche and distal root meristem, we propose that PDR2 and LPR1 function together in an ER-resident pathway that adjusts root meristem activity to external Pi. Our data indicate that the Pi-conditional root phenotype of *pdr2* is not caused by increased Fe availability in low Pi; however, Fe homeostasis modifies the developmental response of root meristems to Pi availability.

multicopper oxidase | P5-type ATPase | phosphate deficiency | root development | SCARECROW

Plant productivity critically depends on postembryonic development of the root system. Dynamic remodeling of root architecture to fluctuating soil conditions is accomplished by adjustment of primary root growth and lateral root formation. Whereas the sensory mechanisms that monitor nutrient availability and optimize root development remain to be elucidated, major players of the intrinsic pathways controlling root patterning and meristem activity have been identified (1–3). The *Arabidopsis* root comprises 3 concentric cell layers (epidermis, cortex, endodermis) surrounding the vascular cylinder (stele). A distal organizer, the quiescent center (QC), maintains stem-cell status of its adjoining undifferentiated cells (initials) whose proximal descendents give rise to differentiated tissue layers after passage through the cell division and elongation zone. The position and functionality of the root stem-cell niche depends on the combinatorial, and in part noncell-autonomous, action of key transcription factors such as SHORT ROOT (SHR), SCARECROW (SCR), and PLETHORA (PLT1/2) (3, 4). Several plant hormones have been implicated in the maintenance of root meristem activity and could mediate growth responses to edaphic cues (4).

Phosphate (Pi) constitutes a major nexus in metabolism and its bioavailability directly impacts plant performance (5, 6). To cope with Pi shortage, often a result of complex soil chemistries (7), plants redesign root system architecture to accelerate soil exploration. In *Arabidopsis*, Pi limitation attenuates primary root growth and stimulates lateral root formation, which is thought to maximize Pi acquisition in the topsoil (8, 9). A genetic approach to dissect Pi sensing identified *Arabidopsis* mutants (10, 11) and accessions (12, 13) with altered sensitivity to the inhibitory effect of Pi deprivation on primary root growth. Characterization of a major quantitative trait locus for root length, *low phosphate root 1* (*lpr1*), revealed a role for multicopper oxidases (LPR1, LPR2) in Pi sensing at the root tip (13, 14). We previously described *phosphate deficiency response 2* (*pdr2*) that displays a hypersensitive response of root meristems to low Pi (10). Here, we show that *PDR2* encodes the P_5-type ATPase and is required for maintaining SCR protein during Pi deprivation, revealing a link between root patterning and the adjustment of meristem activity to Pi availability. Interestingly, *PDR2* and *LPR1* interact genetically, and both proteins are expressed in overlapping cell types of the root tip and are localized to the endoplasmic reticulum (ER). Our analyses of *pdr2* and *lpr1* growth responses further uncover previously described complex interactions between Pi and Fe homeostasis (14–17). We propose that PDR2 and LPR1 are components of an ER-resident pathway mediating root growth responses to Pi and Fe availability.

Results

Loss of *PDR2* Alters Pi Sensitivity of Root Growth Independent of Fe Availability. Attenuation of primary root growth is a developmental response of wild type to Pi limitation, which is exaggerated in *pdr2* plants challenged by low (<100 μM) Pi (10). Because root growth inhibition in −Pi may be a consequence of increased Fe availability and its presumed toxicity (15, 16), we studied the effect of decreasing Fe on Pi-limited root growth and observed that *pdr2* seedlings continue to display the characteristic short-root phenotype at Fe supplementation as low as 1 μM [see Fig. S1*A*]. Further Fe restriction and chelation of residual Fe in the −Pi medium partially rescues the *pdr2* root phenotype, which prompted us to compare Pi dose responses under conditions where a given concentration of Fe^{2+} is bioavailable at each Pi concentration tested (0–2.5 mM Pi). We used the Visual Minteq program (15, 17) to calculate the free Fe^{2+} concentration corresponding to 10 μM $FeSO_4$ in −Pi medium ($\approx$8.8 μM Fe^{2+}) and the appropriate $FeSO_4$ adjustments required to maintain this free Fe^{2+} concentration at different Pi levels. In this controlled Fe condition, primary root growth of *pdr2* shows the reported biphasic Pi dose response (10): A strong inhibition below 0.1 mM Pi and wild type-like growth above this threshold (Fig. S1*B*). Thus, the *pdr2* mutation sensitizes primary root growth to the inhibitory effect of Pi deprivation, which is essentially independent of external Fe availability.

Author contributions: C.A.T., L.N., T.D., and S.A. designed research; C.A.T., R.D.L., S.S., A.W.A., A.C., T.D., and S.A. performed research; C.A.T., R.D.L., S.S., A.W.A., A.C., T.D., and S.A. analyzed data; and C.A.T. and S.A. wrote the paper.

The authors declare no conflict of interest.

This article is a PNAS Direct Submission.

Freely available online through the PNAS open access option.

[1]To whom correspondence should be addressed. E-mail: sabel@ucdavis.edu.

This article contains supporting information online at www.pnas.org/cgi/content/full/0901778106/DCSupplemental.

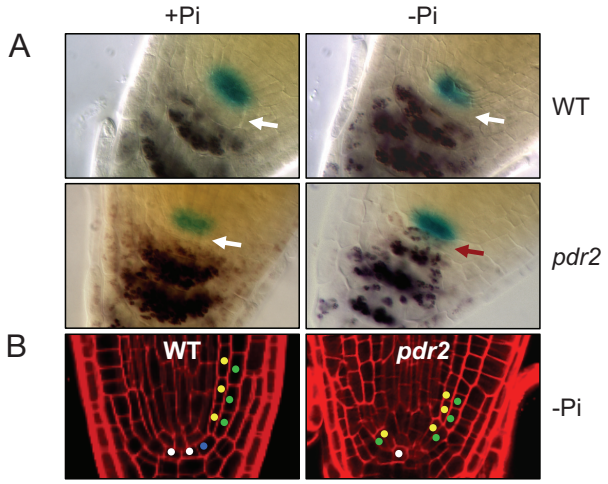

Fig. 1. Loss of stem-cell fate in Pi-deprived *pdr2* roots. Stem-cell identity in primary roots after transfer (2 days) to media containing 2 mM Pi (+Pi) or no Pi supplement (−Pi). (*A*) Double staining of QC (QC25) and columella cells (amyloplasts). White arrows point to the position of columella initials, which show signs of differentiation for *pdr2* after transfer to −Pi (red arrow). (*B*) Optical sections of a root meristem after transfer to −Pi, revealing the absence in *pdr2* roots of cortical/endodermal initials (blue dots) between the QC (white dots) and the endodermis (yellow dots)/cortex (green dots).

***PDR2* Maintains Stem-Cell Fate in Pi-Deprived Roots.** After 5 days of transfer to −Pi medium, wild-type root tips show a slight decrease in *pCYCB1;1*::*GUS* expression, a reporter for cell division (18), and a moderate increase of *pACP5*::*GUS* activity, a marker for Pi starvation and cell differentiation (19). In contrast, only 2–3 days after transfer, root tips of *pdr2* display a sharp decline in *pCYCB1;1*::*GUS* expressing cells and an expanded *pACP5*::*GUS* domain (Fig. S2 *A* and *B*). To explore the cause of meristem exhaustion in *pdr2*, we examined the integrity of the stem-cell niche upon transfer to −Pi by monitoring the expression of QC marker genes as well as the identity of columella initials. In *pdr2*, QC25 expression is detected for over 3 days, although a significant reduction in meristem size is already evident at day 2 (Fig. S2*C*). Similar results were obtained for QC184, suggesting that meristem failure in *pdr2* is at least initially independent of QC identity. Iodine staining revealed amyloplast formation in the layer of columella initials in *pdr2* between 1–2 days after transfer, indicating stem-cell differentiation (Fig. 1*A*). Optical sections further indicated loss of cortex/endodermal initials in *pdr2* (Fig. 1*B*). Thus, *PDR2* is required for root stem-cell maintenance when external Pi is limiting.

***PDR2* Encodes the P_5-Type ATPase.** A map-based strategy identified *PDR2* to encode the single P_5-type ATPase (At5g23630). The EMS-induced *pdr2–1* mutation alters an invariant Thr to an Ile residue in a conserved motif involved in ATP binding (Fig. S3). Two T-DNA insertion lines (*pdr2–2*; *pdr2–3*) show the characteristic root phenotype as well as reduced fertility; the latter phenotype was reported for T-DNA knockouts designated as *male gametogenesis impaired anthers* (*mia*) alleles (20). All phenotypes of *pdr2–1* are complemented with a 10-kb fragment of the wild-type At5g23630 locus (Fig. S4 *A–E*). Overexpression of PDR2 (*p35S*::*PDR2*) increased primary root length in −Pi by ≈35% relative to wild type, rendering root growth essentially insensitive to Pi limitation (Fig. S4 *F* and *G*). In situ hybridization revealed high expression in the central meristematic region as well as weaker signals in the distal meristem and transition zone, which was not observed in *pdr2–2* roots. Analysis of *pPDR2*::*GUS* expression confirmed these results (Fig. 2*A*). Transverse cross-sections revealed *PDR2* promoter activity in all cell types of the root meristem. GUS expression was also detected in pavement cells of trichomes, stipules, stamens, and pollen grains (Fig. 2*B*). The *PDR2* expression patterns are consistent with the morphological phenotypes of *pdr2*/*mia* mutants.

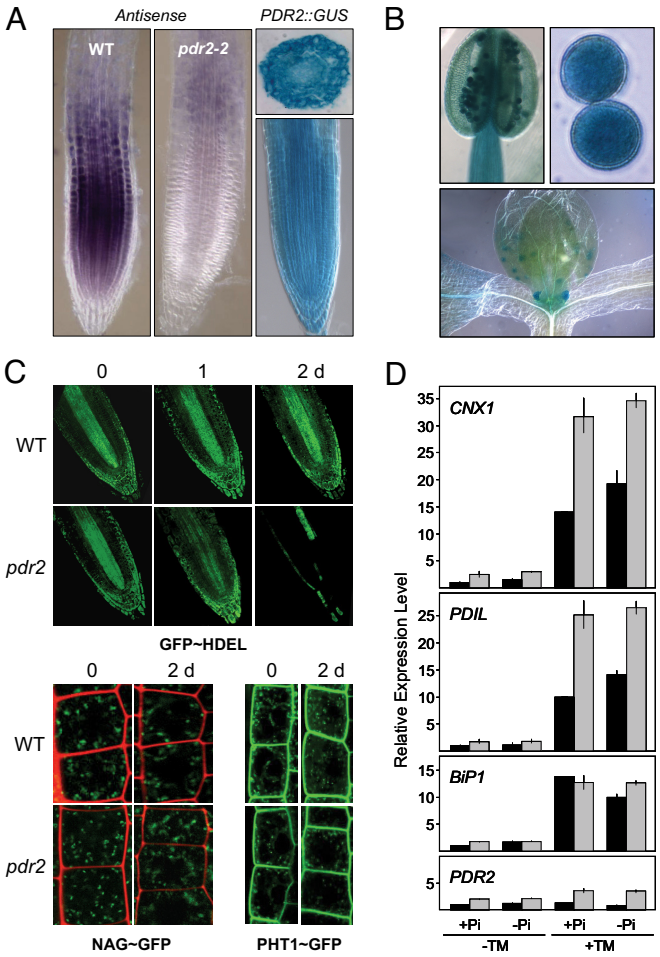

Fig. 2. Expression of *PDR2* and its function in the ER. (*A*) Whole-mount in situ hybridization of *PDR2* in WT and *pdr2–2* primary root tips (antisense probe) and histochemical staining of *pPDR2*::*GUS* expression in a primary root tip (*Lower Right*) and a transverse cross section (*Upper Right*). (*B*) *pPDR2*::*GUS* expression in anthers (*Left*), mature pollen (*Right*) and shoot apex (*Lower*). (*C*) Expression of markers for the ER (*p35S*::*sGFP*~*HDEL*), Golgi (*p35S*::*NAG*~*GFP*) and the plasma membrane (*p35S*::*PHT1;1*~*GFP*) in root tips after germination (5 days) on +Pi medium and subsequent transfer to −Pi (0–2 days). Loss of GFP~HDEL fluorescence is evident in *pdr2* roots after 2 days in −Pi. (*D*) qRT-PCR analysis of *PDR2* and *UPR* gene expression in roots of wild-type (black bars) and *pdr2* (gray bars) after transfer to +Pi or −Pi media in the presence or absence of 5 μM TM for 6 h.

PDR2 Functions in the ER. Because the *Arabidopsis* P_5-type ATPase resides in the ER (20, 21), we tested whether loss of PDR2 impairs the secretory pathway by monitoring markers for the ER [GFP~HDEL (22)], Golgi [NAG~GFP (23)] and plasma membrane [PHT1;1~GFP (24)] (Fig. 2*C*). The subcellular localization of PHT1;1~GFP and NAG~GFP was similar for wild type and *pdr2* root meristems after transfer to −Pi, suggesting that PDR2 inactivation does not disrupt general protein secretion. However, exposure to −Pi caused within 2 days a substantial decline in GFP~HDEL fluorescence in *pdr2* but not wild-type root meristems. The GFP~HDEL reporter was used to study ER-associated protein degradation (ERAD) in plants, which is 1 mechanism to control protein quality in the secretory pathway (25). Loss of GFP~HDEL expression in Pi-limited *pdr2* roots suggests sensitization of ER quality control mechanisms, which also include activation of unfolded response genes (*UPR*) genes. We examined

expression of *PDR2* and select *UPR* genes in response to altered Pi availability and treatment with tunicamycin (TM), a potent UPR inducer (Fig. 2*D*). *PDR2* mRNA expression did not appreciably change in response to −Pi or +TM treatment. Whereas expression of *CNX1*, *PDIL*, or *BiP1* was ≈2-fold higher in Pi-sufficient *pdr2* roots relative to wild type, transfer to −Pi marginally increased (<2-fold) transcript levels in either genotype. As expected, a strong induction (≈10-fold) was evident for wild type during transfer from +Pi to +Pi/+TM medium. Interestingly, expression of *CNX1* and *PDIL* mRNA was notably higher for *pdr2* roots (>20-fold). Transfer from +Pi to −Pi/+TM medium did not further elevate *UPR* gene expression (Fig. 2*D*). Collectively, our data indicate that loss of PDR2 sensitizes a subset of ER quality control responses.

PDR2 Restricts SHR Movement in Limiting Pi. Because PDR2 is necessary for stem-cell maintenance in low Pi, we determined transcript levels of 6 root patterning genes in wild-type and *pdr2* roots for up to 2 days after transfer to −Pi, but observed only changes smaller than 2-fold (Fig. S5*A*). A function of PDR2 in the secretory pathway prompted us to examine whether SHR protein expression and localization is altered in *pdr2* root meristems because radial root patterning depends on SHR trafficking from the stele into the endodermis (26). As expected, *SHR* promoter activity (*pSHR*::YFP_{NLS}) was not affected in Pi-limited wild type and *pdr2* roots (Fig. S5*B*). However, although SHR∼GFP protein expression (*pSHR*::*SHR∼GFP*) did not change in wild type root meristems during 2 days of Pi shortage, SHR∼GFP fluorescence initially declined in the endodermal cell layer of *pdr2* roots at day 1 and noticeably decreased in the stele at day 2 after transfer (Fig. 3). Loss of SHR∼GFP could be the result of accelerated protein degradation; however, we detected ectopic SHR∼GFP fluorescence in cortex and epidermal cells, suggesting unrestricted SHR movement into adjacent cell layers of Pi-deprived *pdr2* roots (Fig. 3, insets), as was previously reported for lines with reduced *SCR* expression (27).

PDR2 Maintains SCR Level in Limiting Pi. Because SCR directly interacts with SHR in endodermal cell nuclei and restricts further SHR movement (27), we monitored GFP∼SCR expression and used complemented *scr-4* (*pSCR*::*GFP*∼SCR) to introgress the reporter into *pdr2*. Whereas GFP∼SCR expression and root meristem organization did not change in the wild type ($PDR2^{+/+}$*scr-4*$^{-/-}$*GFP∼SCR*$^{+/+}$) for at least 2 days after transfer to −Pi, both traits were strikingly altered for *pdr2* in a *SCR* dose-dependent manner (Fig. 4*A*). We identified homozygous *pdr2* lines harboring 1–4 *SCR* alleles, with at least 1 *GFP∼SCR* copy. When grown in +Pi, GFP∼SCR expression in *pdr2* was similar to the wild type. In *pdr2* (1x*SCR*), GFP∼SCR expression was largely abolished within 1 day after transfer to −Pi. A single cell layer of ground tissue was often observed at day 2 (32 of 41 seedlings), which is characteristic of *scr* and *shr* roots (28). GFP∼SCR fluorescence in newly emerged lateral root meristems was still detectable, as was J0571 expression, a GFP marker for cortex and endodermis (Fig. S5*C*). In *pdr2* (2× *SCR*), GFP∼SCR expression was greatly reduced at day 1 and only residual fluorescence was detected in the primary meristem at day 2, which showed signs of disorganization. As expected, immunoblot analysis revealed reduction of authentic SCR protein in Pi-deprived *pdr2* roots, which was not observed for wild-type or Pi-sufficient seedlings (Fig. 4*B*). In *pdr2* (3× *SCR*), GFP∼SCR expression was less reduced even 2 days after transfer. GFP∼SCR fluorescence appeared also in the cortex and ectopic cell divisions in the ground tissue were frequently observed (48 of 67 seedlings). Surprisingly, GFP∼SCR expression was maintained in *pdr2* (4× *SCR*) lines for 4–5 days after transfer. Although loss of the stem-cell niche was initially prevented, the proximal meristem showed signs of cell differentiation, and these roots ultimately displayed a short root phenotype in −Pi.

The rescue of distal meristem activity in Pi-deprived *pdr2* (4× *SCR*) roots and ensuing proximal meristem reduction points to a dual function of PDR2 in Pi-dependent root meristem maintenance, which is also indicated by the analysis of the *pdr2–1 scr-3* double mutant (Fig. S6). Primary roots of *pdr2 scr* seedlings display the *pdr2* phenotype on −Pi and respond like *pdr2* to decreasing Pi availability. However, meristem organization of the double mutant is indistinguishable from *scr* on −Pi, revealing the characteristic single ground cell layer, which is reminiscent of Pi-starved *pdr2* (1× *SCR*) roots (Fig. 4*A*). Thus, PDR2 is required for maintaining SCR expression in the stem-cell niche as well as for proximal meristem activity under Pi limitation.

The ER Participates in Root Meristem Response to Pi Deficiency. It is not clear how ER-resident PDR2 maintains nuclear SCR level when Pi is limiting. However, we observed an uncharacteristic GFP∼SCR localization in a substantial fraction of endodermal cells of wild-type roots harboring extra (3 or 4) *SCR* copies (Fig. 5*A*). In addition to its expected nuclear localization, GFP∼SCR fluorescence was detected throughout the cell in a pattern consistent with the endomembrane system. ER localization of GFP∼SCR was confirmed by counterstaining with ER-Tracker and further corroborated by its sensitivity to TM, which caused rapid loss of GFP∼SCR fluorescence only in wild-type roots with extra *SCR* copies (Fig. 5*A*). This observation raises the possibility that nuclear SCR level depends on ER-associated activities, which is further suggested by the effect of brefeldin A (BFA) on *pdr2* root meristems. BFA reversibly inhibits vesicle trafficking and induces redistribution of Golgi proteins into the ER (29). When compared to wild type on +Pi, primary root growth of *pdr2* is strongly inhibited by 5 μM BFA. BFA also inhibits root growth of wild type on −Pi, with no additional effect on *pdr2* (Fig. S7). Reduction of *pdr2* root meristem size by BFA treatment in +Pi is illustrated by loss of GFP∼SCR and *pCYCB1;1*::*GUS* expression (Fig. 5*B*), which is reminiscent of Pi-deprived *pdr2* root meristems (Fig. 4*A* and Fig. S2*A*). Thus, BFA treatment of Pi-sufficient *pdr2* roots mimics the effect of Pi deficiency.

LPR1 Interacts Genetically with PDR2 and Localizes to the ER. Overexpression of *PDR2* alleviates the inhibitory effect of Pi deprivation on primary root growth (Fig. S4 *F* and *G*), a phenotype similar to recessive *lpr1* and *lpr2* mutants that develop longer primary roots in −Pi than the wild type (13, 14). To study the relationship between *PDR2* and *LPR* genes, we compared the growth response of wild type, *pdr2*, *lpr1lpr2*, and *pdr2lpr1lpr2* roots to Pi shortage. In −Pi, primary root length and meristem size of *lpr1lpr2* and *pdr2lpr1lpr2* lines were similar and both parameters exceeded those of the wild type (Fig. 6*A*). The nearly full epistasis indicates that loss of *LPR1*/*LPR2* cannot be bypassed by *PDR2* inactivation. Because both predicted LPR multicopper oxidases contain a putative N-terminal signal peptide (SP), we determined the subcellular localization of *p35S*::*SP∼eGFP∼LPR1* expression (Fig. 6*B*). GFP∼LPR1 fluorescence was detected in transgenic *Arabidopsis* root cells in a pattern consistent with a reticular network. Transient co-expression with an ER marker (*p35S*::*DsRed2∼KDEL*) revealed co-localization of both reporter proteins in *N. benthamiana* leaf cells, including the perinuclear intermembrane space (Fig. 6*B*). Thus, the ER-resident LPR enzymes function together with the P_5-type ATPase in a common pathway that adjusts root meristem activity to Pi availability.

Discussion

We show that *PDR2* encodes the single P_5-type ATPase (At5g23630) previously named MIA (20). The *Arabidopsis* family of P-type ATPases consists of 46 members that can be assorted into 5 groups according to their transport ions (heavy metals, Ca^{2+}, H^+, and aminophospholipids) (30). The specificity and precise role of any P_5 pump is unknown (31). Cod1p, the PDR2/MIA ortholog in yeast (*S. cerevisiae*), is located in the ER and nuclear envelope (32). Properties of *cod1*Δ strains point to

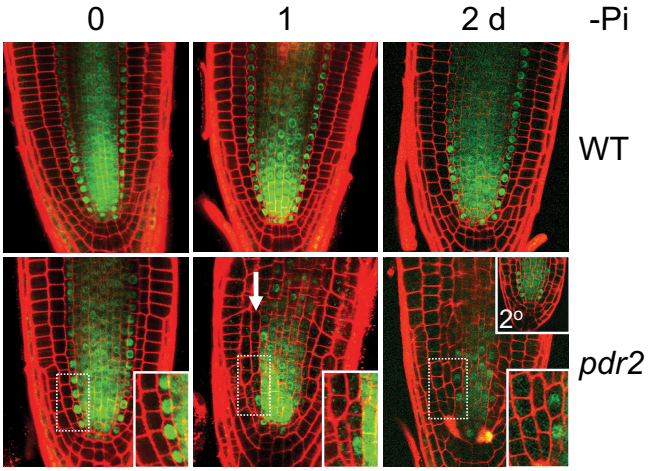

Fig. 3. PDR2 is necessary for maintaining SHR distribution in low Pi. Transgenic WT and *pdr2–1* seeds were germinated on +Pi medium (5 days) and *pSHR::SHR~GFP* expression was monitored after transfer to −Pi (0–2 days). The arrow points to the endodermal cell layer. Lower insets show enlarged images of framed areas. The upper inset shows a newly emerged lateral root.

its function in protein biogenesis and ER quality control, including protein processing, control of protein insertion orientation, ERAD, and cation homeostasis (33–36). Several observations support a role for PDR2/MIA in the ER: (*i*) its C-terminal ER retrieval signal of the KKXX-type suggests retrograde Golgi-to-ER transport (37); (*ii*) a proteomics approach identified the At5g23630 protein in ER microsomes (21); and (*iii*) Jakobsen et al. (20) detected MIA by immunogold labeling in the ER and small vesicles in tapetal cells and demonstrated its ability to complement *cod1*Δ. Disruption of *MIA* deregulates gene expression related to protein folding and secretion in anthers, suggesting enhanced protein quality control and reduced ER protein load, whereas changes in transcript levels of solute transporter genes likely cause cation imbalances in *mia* leaves (20). We show that loss of *PDR2/MIA* selectively sensitizes *UPR* gene expression in roots (Fig. 2*D*). General secretion is not severely compromised in *pdr2* root meristems (Fig. 2*C*), which is supported by our previous report that Pi-starved *pdr2* roots secrete higher activities of phosphohydrolases than the wild type, likely as a consequence of elevated expression of Pi starvation-inducible genes (10) (Fig. S5*A*).

PDR2 is required for maintaining nuclear SCR protein when Pi is limiting (Fig. 4*A*), a failure of which causes stem-cell differentiation (Fig. 1) and meristem reduction (Fig. S2). SCR and SHR are members of the GRAS family of transcription factors and key regulators of radial root patterning. SCR is normally expressed in the QC, cortex/endodermal initials and endodermis, and at low level in the cortex (38, 39). *SHR* transcription is restricted to the stele, but the SHR protein moves into the adjacent cell layer where it activates *SCR* transcription and controls endodermis specification (26). SCR delimits SHR movement by direct protein interaction and SCR/SHR-dependent autoactivation of *SCR* transcription. Interestingly, RNAi-mediated reduction of *SCR* expression allows unsequestered SHR to pass into the presumptive cortex where it activates *SCR* and ectopic endodermis specification (27). Our data suggest that PDR2 inactivation causes rapid reduction of SCR protein in low Pi (within 1 day), which can be compensated by increasing *SCR* gene dosage. In Pi-starved *pdr2* roots harboring only 1 or 2 *SCR* copies, SCR level is possibly too low to confine SHR in the endodermis and to trigger SCR/SHR-dependent *SCR* upregulation (Fig. 4 *A* and *B*). Thus, the observed loss of SHR~GFP fluorescence in the endodermis in −Pi (Fig. 3) is likely a consequence of unhindered SHR~GFP movement into peripheral cell

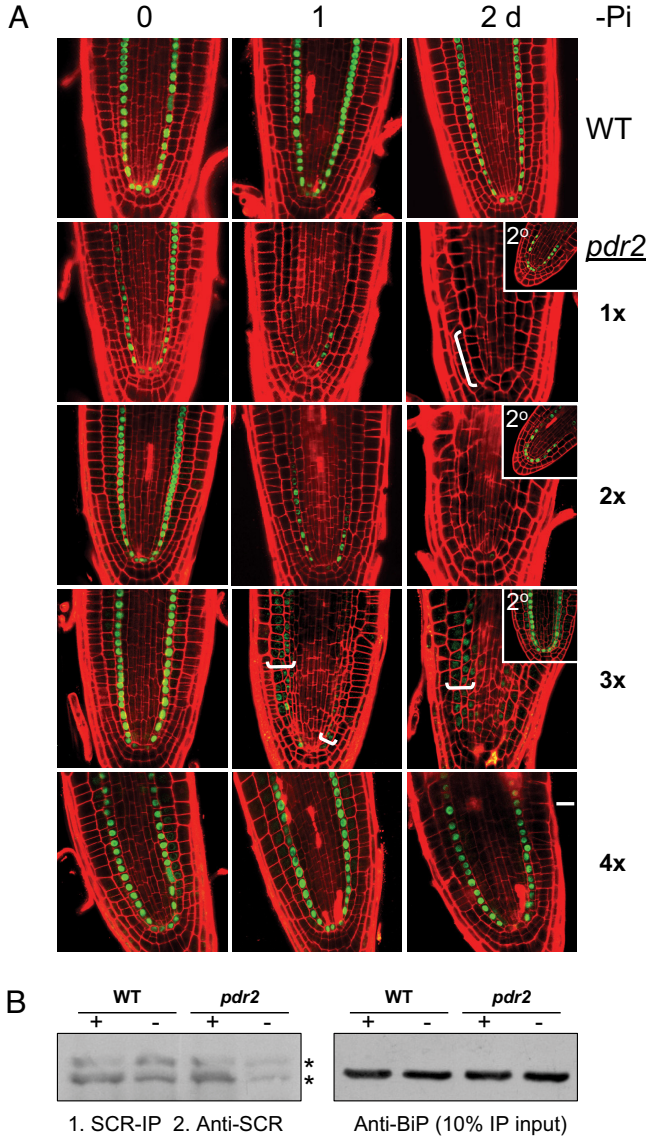

Fig. 4. PDR2 is necessary for maintaining SCR protein level in low Pi. (*A*) *pSCR::GFP~SCR* expression in root meristems of WT and *pdr2–1* harboring 1–4 alleles of *SCR* (1–4×), with at least 1 copy of the GFP~SCR reporter. Transgenic WT and *pdr2* seeds were germinated on +Pi medium (5 days) and transferred to −Pi (0–2 days). The white bracket for *pdr2* (1× *SCR*) outlines a single layer of ground tissue characteristic of *shr* and *scr* mutants. White brackets for *pdr2* (3× *SCR*) indicate supernumerary endodermal cells displaying GFP~SCR fluorescence similar to *SCR* RNAi lines (27). Insets show newly emerged lateral roots. The white bar for *pdr2* (4× *SCR*) denotes the proximal meristem border. (*B*) Endogenous SCR level in root extracts of WT and *pdr2* after transfer to +Pi or −Pi (2 days). *Left* shows anti-SCR immunoblot of SCR-IP. *Right* shows anti-BiP immunoblot of 10% SCR-IP input.

layers. In *pdr2* (3× *SCR*) roots, SCR may approach a level closer to wild-type threshold, which still permits continued SHR movement but is already sufficient to activate SCR/SHR-dependent *SCR* transcription in recipient cell files. Threshold is restored or exceeded in *pdr2* (4× *SCR*) roots that show wild type-like GFP~SCR expression in the distal meristem (Fig. 4*A*). Thus, the *pdr2* mutation strikingly mimics in −Pi the effect of RNAi-mediated SCR reduction (27). However, PDR2 inactivation likely affects nuclear SCR protein level posttranscriptionally because steady-state *SCR* and *SHR* mRNA levels in roots do not respond to Pi deprivation (Fig. S5).

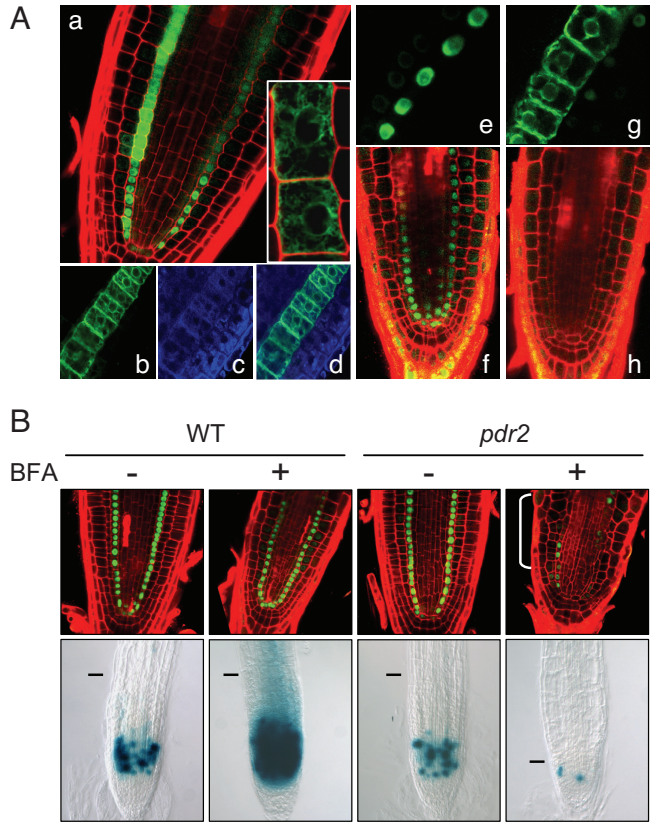

Fig. 5. A role of the secretory pathway for root meristem maintenance. (*A*) Increased *SCR* dosage results in localization of GFP∼SCR to the ER in wild type. Optical sections of WT root tips harboring 3 *SCR* copies (a–d). Inset in (a) indicates endodermal cells at higher magnification. GFP∼SCR (b) co-localizes with ER tracker DPX fluorescence (c and d). GFP∼SCR fluorescence in wild type with 2 (e and f) or 3 *SCR* copies (g and h) before (e and g) and after (f and h) tunicamycin treatment (5 μM, 4 h). (*B*) BFA mimics the effects of −Pi on *pdr2* root meristems in Pi sufficiency. (*Upper*), *pSCR*::*GFP*∼*SCR* expression in roots following transfer to +Pi media with or without 25 μM BFA (1 day). The white bracket outlines meristem size reduction. (*Lower*), *pCYCB1*::*GUS* expression in 14-day-old primary root tips of WT and *pdr2* seedlings grown in +Pi media in the absence (−) or presence (+) of 10 μM BFA.

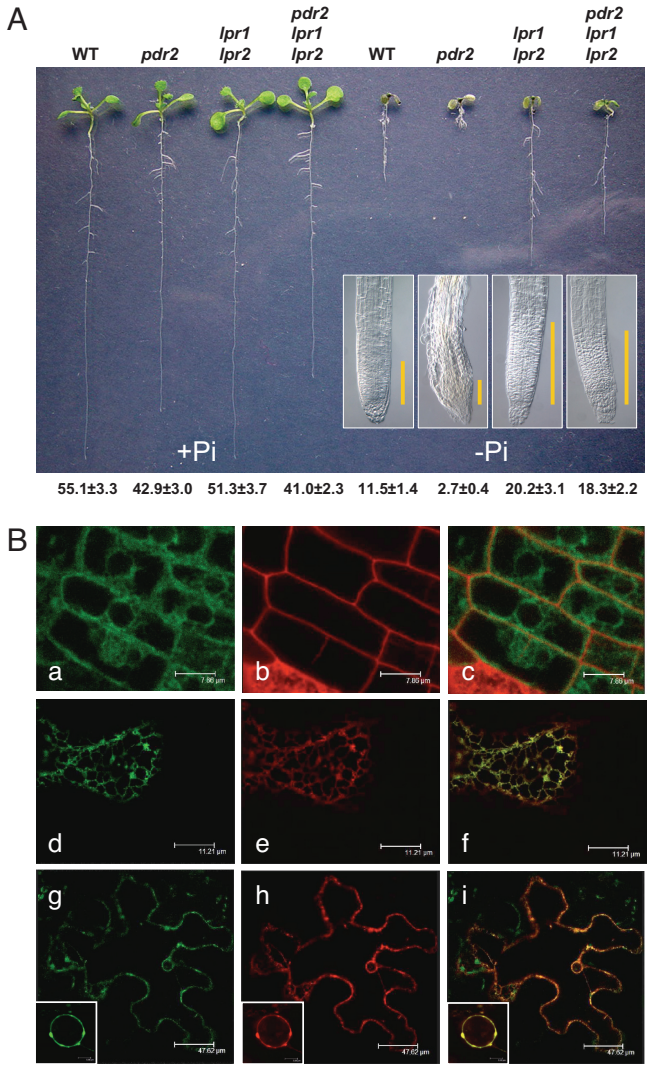

Fig. 6. *LPR* genes functionally interact with *PDR2* and encode ER proteins. (*A*) Loss of *LPR1* and *LPR2* rescues the *pdr2* root phenotype in low Pi. The mean primary root length (mm) of seedlings grown for 8 day in +Pi or −Pi medium (± SD, $n = 10$–15) is given below. *Insets* show cleared root tips of seedlings grown in −Pi. The approximate size of primary meristems is indicated by yellow bars. (*B*) Subcellular localization of LPR1. Expression of *p35S*::*SP*∼*eGFP*∼*LPR1* in stably transformed *Arabidopsis* root tips: (a) GFP∼LPR1 fluorescence, (b) propidium iodide staining, and (c) overlay. Transient co-expression of *p35S*::*SP*∼*eGFP*∼*LPR1* and *p35S*::*DsRed2*∼*KDEL* in epidermal leaf cells of *N. benthamiana*: (d, g) GFP∼LPR1 fluorescence, (e and h) DsRed2∼KDEL fluorescence, (f and i) overlays. *Insets* (g–i) show close-up of the cell nucleus.

Several observations suggest that endosomal compartments participate in regulating nuclear SCR level: (*i*) increased *SCR* gene dosage in wild type can cause atypical GFP∼SCR localization to the ER (Fig. 5*A*); (*ii*) BFA treatment of Pi-sufficient *pdr2* roots mimics the effect of low Pi on GFP∼SCR expression (Fig. 5*B*); (*iii*) SCR physically interacts with a SEC14 family member of phospholipid transfer proteins (40), which regulate membrane trafficking in yeast (41); and (*iv*) the GRAS domain of SCR has the capacity to mediate cell-to-cell movement (39). The unknown biochemical activity of P_5-type ATPases and the diverse molecular phenotypes of *Arabidopsis* and yeast knockouts leave open the question how PDR2 maintains SCR in low Pi. Although the mechanism is most likely indirect, for example, by maintaining ER ion homeostasis, specific PDR2-dependent activities of the early secretory pathway may regulate SCR level. For example, the key enzyme of the mevalonate pathway, HMG-CoA reductase, is feedback-regulated via ERAD in yeast, and loss of Cod1p causes its constitutive degradation without promoting removal of other ER proteins (32, 33). Because SCR down-regulates RBR (RETINOBLASTOMA-RELATED) in the stem-cell niche (42), PDR2-dependent growth response to Pi status likely impinges on the SCR-RBR pathway to adjust the balance of cell division and differentiation in the root meristem.

A role of the ER in root growth response to external Pi status is further supported by the subcellular localization of LPR1 and its genetic interaction with PDR2 (Fig. 6). The expression domains of *LPR1* (14) and *PDR2* (Fig. 2*A*) overlap in the stem-cell niche and distal root meristem, suggesting that both proteins function together in an ER-resident pathway that adjusts meristem activity to external Pi status. Because the recessive *lpr1lpr2* and *pdr2* mutations result in opposite phenotypes in low Pi and *lpr1lpr2* is epistatic to *pdr2*, the P_5-type ATPase likely restricts LPR output, either by negatively regulating LPR biogenesis or activity, or by removing products generated by LPR multicopper oxidases (Fig. S8). It has recently been argued that root growth inhibition by limiting Pi is rather an indirect result of elevated Fe availability and its presumed toxicity than a consequence of Pi shortage (15). We observed that *pdr2* root growth is hypersensitive to change in external Pi even

under controlled Fe conditions and is essentially unaffected by reduction of the Fe supplement to as low as 1 μM; however, further Fe restriction or chelation of residual Fe in the −Pi medium substantially rescues the *pdr2* root phenotype (Fig. S1*A*). Thus, the *pdr2* mutation sensitizes root growth response to both external Pi and Fe. Because Pi deprivation causes elevated Fe tissue content and regulates genes affecting Fe homeostasis (16, 17), our data on PDR2 and LPR1 are consistent with a model in which Pi availability interacts with Fe homeostasis to adjust root meristem activity via proteins of the ER and cell nucleus (Fig. S8).

Materials and Methods

Plant Material and Growth Conditions. *Arabidopsis* lines were grown on 0.8% phytagar containing 0.5% sucrose and 0.5× MS salts with (+Pi) or without (−Pi) 0.625 mM KH_2PO_4, pH 5.6. For media with altered Pi and/or Fe content, the previously described MS-based salt composition was used (10). Nutrient bioavailability was calculated by using the Visual Minteq program (15). See *SI Text* for details.

Identification of *PDR2*. The *PDR2* locus was mapped to chromosome 5 between markers CER 460453 and CER 456861. This region was sequenced and the *pdr2–1* point mutation verified by molecular complementation (*SI Text*).

Microscopy. Roots were cleared and imaged with DIC optics (Zeiss Axioskop). For confocal microscopy, roots were counterstained in 10 μM propidium iodide and imaged (Olympus FV-1000 or Leica SP2 AOBS). Transient assays of *p35S::SP∼eGFP∼LPR1* and *p35S::DsRed2∼KDEL* co-expression were performed as described (*SI Text*).

qRT-PCR. Gene expression analysis was performed by qRT-PCR by using the 7300 Real-Time PCR System (Applied Biosystems), SYBR Green I PCR master mix, and the amplimers listed in Tables S1 and S2. Data were analyzed by the $\Delta\Delta$-C_T method (*SI Text*).

Co-Immunoprecipitation Analysis. Endogenous SCR protein level was detected as described (27) (*SI Text*).

ACKNOWLEDGMENTS. We thank B. Scheres and R. Heidstra (University of Utrecht, The Netherlands), P. Benfey (Duke University, Durham, NC), I. Moore (University of Oxford, Oxford), and J. Paz-Ares (Centro Nacional de Biotecnologia, Madrid, Spain) for transgenic lines; P. Benfey for SCR antibody; V. Rubio (Centro Nacional de Biotecnologia, Madrid, Spain) and R. Bhat (Commisariat al'Energie Atomique Cadarache) for plasmids; and C. Arnaud (Commisariat a l'Energie Atomique Cadarache) for initiating construction of *pdr2lpr1lpr2* lines. We further thank B. Scheres for discussion and J. Harada for critical comments. This work was supported by U.S. Department of Energy Grant DE-FG0203ER15447 (to S.A.). A.C., L.N., and T.D. were supported by the Commissariat à l'Energie Atomique.

1. Malamy JE (2005) Intrinsic and environmental response pathways that regulate root system architecture. *Plant Cell Environ* 28:67–77.
2. Osmont KS, Sibout R, Hardtke CS (2007) Hidden branches: Developments in root system architecture. *Annu Rev Plant Biol* 58:93–113.
3. Petricka JJ, Benfey PN (2008) Root layers: Complex regulation of developmental patterning. *Curr Opin Genet Dev* 18:354–361.
4. Iyer-Pascuzzi AS, Benfey PN (2009) Transcriptional networks in root cell fate specification. *Biochim Biophys Acta* 1789:315–325.
5. Schachtman DP, Shin R (2007) Nutrient sensing and signaling: NPKS. *Annu Rev Plant Biol* 58:47–69.
6. Ticconi CA, Abel S (2004) Short on phosphate: Plant surveillance and countermeasures. *Trends Plants Sci* 9:548–555.
7. Raghothama KG (1999) Phosphate acquisition. *Annu Rev Plant Physiol Plant Mol Biol* 50:665–693.
8. Desnos T (2008) Root branching responses to phosphate and nitrate. *Curr Opin Plant Biol* 11:82–87.
9. Lopez-Bucio J, Cruz-Ramirez A, Herrera-Estrella L (2003) The role of nutrient availability in regulating root architecture. *Curr Opin Plant Biol* 6:280–287.
10. Ticconi CA, Delatorre CA, Lahner B, Salt DE, Abel S (2004) *Arabidopsis pdr2* reveals a phosphate-sensitive checkpoint in root development. *Plant J* 37:801–814.
11. Sanchez-Calderon L, et al. (2006) Characterization of *low phosphorus insensitive* mutants reveals a crosstalk between low phosphorus-induced determinate root development and the activation of genes involved in the adaptation of *Arabidopsis* to phosphorus deficiency. *Plant Physiol* 140:879–889.
12. Chevalier F, Pata M, Nacry P, Doumas P, Rossignol M (2003) Effects of phosphate availability on the root system architecture: Large-scale analysis of the natural variation between *Arabidopsis* accessions. *Plant Cell Environ* 26:1839–1850.
13. Reymond M, Svistoonoff S, Loudet O, Nussaume L, Desnos T (2006) Identification of QTL controlling root growth response to phosphate starvation in *Arabidopsis thaliana*. *Plant Cell Environ* 29:115–125.
14. Svistoonoff S, et al. (2007) Root tip contact with low-phosphate media reprograms plant root architecture. *Nat Genet* 39:792–796.
15. Ward JT, Lahner B, Yakubova E, Salt DE, Raghothama KG (2008) The effect of iron on the primary root elongation of *Arabidopsis* during phosphate deficiency. *Plant Physiol* 147:1181–1191.
16. Hirsch J, et al. (2006) Phosphate deficiency promotes modification of iron distribution in *Arabidopsis* plants. *Biochimie* 88:1767–1771.
17. Misson J, et al. (2005) A genome-wide transcriptional analysis using *Arabidopsis thaliana* Affymetrix gene chips determined plant responses to phosphate deprivation. *Proc Natl Acad Sci USA* 102:11934–11939.
18. Colon-Carmona A, You R, Haimovitch-Gal T, Doerner P (1999) Technical advance: Spatio-temporal analysis of mitotic activity with a labile cyclin-GUS fusion protein. *Plant J* 20:503–508.
19. del Pozo JC, et al. (1999) A type 5 acid phosphatase gene from *Arabidopsis thaliana* is induced by phosphate starvation and by some other types of phosphate mobilising/oxidative stress conditions. *Plant J* 19:579–589.
20. Jakobsen MK, et al. (2005) Pollen development and fertilization in *Arabidopsis* is dependent on the male gametogenesis impaired anthers gene encoding a Type V P-type ATPase. *Genes Dev* 19:2757–2769.
21. Dunkley TP, et al. (2006) Mapping the *Arabidopsis* organelle proteome. *Proc Natl Acad Sci USA* 103:6518–6523.
22. Zheng H, Kunst L, Hawes C, Moore I (2004) A GFP-based assay reveals a role for RHD3 in transport between the endoplasmic reticulum and Golgi apparatus. *Plant J* 37:398–414.
23. Xu J, Scheres B (2005) Dissection of *Arabidopsis* ADP-ribosylation factor 1 function in epidermal cell polarity. *Plant Cell* 17:525–536.
24. Gonzalez E, Solano R, Rubio V, Leyva A, Paz-Ares J (2005) Phosphate transported traffic facilitator 1 is a plant-specific sec12-related protein that enables the endoplasmic reticulum exit of a high-affinity phosphate transporter in *Arabidopsis*. *Plant Cell* 17:3500–3512.
25. Brandizzi F, et al. (2003) ER quality control can lead to retrograde transport from the ER lumen to the cytosol and the nucleoplasm in plants. *Plant J* 34:269–281.
26. Helariutta Y, et al. (2000) The short-root gene controls radial patterning of the *Arabidopsis* root through radial signaling. *Cell* 101:555–567.
27. Cui H, et al. (2007) An evolutionarily conserved mechanism delimiting SHR movement defines a single layer of endodermis in plants. *Science* 316:421–425.
28. Nakajima K, Sena G, Nawy T, Benfey PN (2001) Intercellular movement of the putative transcription factor SHR in root patterning. *Nature* 413:307–311.
29. Mossessova E, Corpina RA, Goldberg J (2003) Crystal structure of ARF1*Sec7 complexed with brefeldin A and its implications for the guanine nucleotide exchange mechanism. *Mol Cell* 12:1403–1411.
30. Baxter I, et al. (2003) Genomic comparison of P-type ATPase ion pumps in *Arabidopsis* and rice. *Plant Physiol* 132:618–628.
31. Moller AB, Asp T, Holm PB, Palmgren MG (2008) Phylogenetic analysis of P5 P-type ATPases, a eukaryotic lineage of secretory pathway pumps. *Mol Phylogenet Evol* 46:619–634.
32. Cronin SR, Rao R, Hampton RY (2002) Cod1p/Spf1p is a P-type ATPase involved in ER function and $Ca2^+$ homeostasis. *J Cell Biol* 157:1017–1028.
33. Cronin SR, Khoury A, Ferry DK, Hampton RY (2000) Regulation of HMG-CoA reductase degradation requires the P-type ATPase Cod1p/Spf1p. *J Cell Biol* 148:915–924.
34. Suzuki C, Shimma YI (1999) P-type ATPase spf1 mutants show a novel resistance mechanism for the killer toxin SMKT. *Mol Microbiol* 32:813–823.
35. Vashist S, Ng DT (2004) Misfolded proteins are sorted by a sequential checkpoint mechanism of ER quality control. *J Cell Biol* 165:41–52.
36. Tipper DJ, Harley CA (2002) Yeast genes controlling responses to topogenic signals in a model transmembrane protein. *Mol Biol Cell* 13:1158–1174.
37. Stornaiuolo M, et al. (2003) KDEL and KKXX retrieval signals appended to the same reporter protein determine different trafficking between endoplasmic reticulum, intermediate compartment, and Golgi complex. *Mol Biol Cell* 14:889–902.
38. Di Laurenzio L, et al. (1996) The *scarecrow* gene regulates an asymmetric cell division that is essential for generating the radial organization of the *Arabidopsis* root. *Cell* 86:423–433.
39. Gallagher KL, Benfey PN (2009) Both the conserved GRAS domain and nuclear localization are required for short-root movement. *Plant J* 57:785–797.
40. Cui H, Benfey PN (2009) Interplay between SCARECROW, GA and LIKE HETEROCHROMATIN PROTEIN 1 in ground tissue patterning in the *Arabidopsis* root. *Plant J* 58:1016–1027.
41. Chang HJ, Jones EW, Henry SA (2002) Role of the unfolded protein response pathway in regulation of INO1 and in the sec14 bypass mechanism in *Saccharomyces cerevisiae*. *Genetics* 162:29–43.
42. Wildwater M, et al. (2005) The retinoblastoma-related gene regulates stem cell maintenance in *Arabidopsis* roots. *Cell* 123:1337–1349.